Title

An Integrated Approach to Improve the Assay Performance of Quantum Dot-Based Lateral Flow Immunoassays by Using Silver Deposition.

Authors

Wang, Yulong

Liu, Pengyan

Ye, Yuhui

et al.

Publication Date

2023-09-01

DOI

10.1016/j.microc.2023.108932

Peer reviewed

HHS Public Access

Author manuscript

Microchem J. Author manuscript; available in PMC 2024 September 01.

Published in final edited form as:

Microchem J. 2023 September ; 192: . doi:10.1016/j.microc.2023.108932.

An Integrated Approach to Improve the Assay Performance of Quantum Dot-Based Lateral Flow Immunoassays by Using Silver Deposition

Yulong Wang[a,b,c], **Pengyan Liu**[a], **Yuhui Ye**[a], **Bruce D. Hammock**[d], **Cunzheng Zhang**[a,c,e,*]

[a]Key Lab of Food Quality and Safety of Jiangsu Province-State Key Laboratory Breeding Base, Ministry of Agriculture, Institute of Food Safety and Nutrition, Jiangsu Academy of Agricultural Sciences, Nanjing 210014, China

[b]School of the Environment and Safety Engineering, Jiangsu University, Zhenjiang, 212013, China

[c]Anhui Science and Technology University, Fengyang 233100, China

[d]Department of Entomology and Nematology, UCD Comprehensive Cancer Center, University of California, Davis, CA 95616, USA

[e]School of Biology and food engineering, Jiangsu University, Zhenjiang 212013, China

Abstract

Traditional quantum dot-based lateral flow immunoassay (QD-LFIA) is limited to signal loss in part by the blinking, photobleaching and oxidative quenching of QD probes. Inspired by the good application of silver deposition on QD surfaces in tissue imaging, and in the context of improving the assay performance without compromising the simplicity and practicality, we report that introducing the QD-silver combination to the LFIA system, has the advantages of accuracy improvement, signal enhancement and user friendliness promotion, but maintains the cost-effective property and commercial accessibility of QD-LFIA. The effect was shown by using CdSe/ZnS QD-LFIA coupled with anti-sodium pentachlorophenate antibody, which provided a 4-fold improvement in the signal, a 2.5-fold improvement in the detection limit and a zero false-negative rate for sodium pentachlorophenate analysis in chicken samples. The proposed LFIA integrates the possibilities of colorimetric and fluorometric detection with different detection limits (fluorometric at 10 ng/mL and colorimetric at 4 ng/mL) and with acceptable detection times (fluorometric at 12 min and colorimetric at 27 min). The current results indicate that this

*Correspondence: zhcz2003@hotmail.com.

Author Contributions:

Investigation, Methodology, Yulong Wang.; Methodology, Yulong Wang.; Validation, Yuhui Ye.; Formal Analysis, Pengyan Liu.; Data Curation, Yulong Wang.; Writing-Original Draft Preparation, Yulong Wang.; Writing-Review & Editing, Bruce D. Hammock and Cunzheng Zhang.; Supervision, Conceptualization, Funding Acquisition, Project Administration, Cunzheng Zhang.

Supplementary Materials:

Reference methods of HPLC−MS/MS and ELISA for sample analysis. Visualization of LFIA performance of different volumes of QD-protein G (Fig. S1), visualization of LFIA performance of different volumes of SPCmAb (Fig. S2), visualization of LFIA performance of different deposition time of silver (Fig. S3), detection limit of the reagent-limited QD-silver LFIA (Fig. S4), visualization of LFIA performance for simulated signal loss of QD probes under abnormal operating conditions (Fig. S5), and visualization of LFIA performance for chicken samples spiked/ naturally contaminated by SPC (Fig. S6).

Declaration of Competing Interest: The authors declare no conflict of interest.

QD-silver combined LFIA is complementary to conventional fluorescence LFIA and could be an inexpensive, versatile, and sensitive alternative.

Table of contents (TOC)

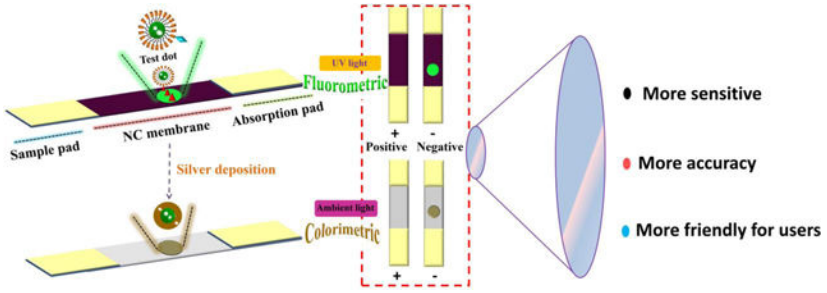

Keywords

Quantum dot; Lateral flow immunoassay; Silver deposition; Sodium pentachlorophenate; Signal enhancement

1. Introduction

The lateral flow immunoassay (LFIA) is extensively applied in analytical biochemistry/chemistry through a number of signal measurement techniques that exploit the great specificity of the immunological reaction and the rapidity of capillary action [1–3]. Currently, LFIA represents a core point-of-care or on-site testing modality for the identification of analytes in many areas ranging from clinical diagnosis, and drug abuse testing to environmental and food safety monitoring. The popular home pregnancy strip and the latest strip kit for COVID-19 detection that uses the lateral flow system provide clear evidence of the value of such a system for portable use of analyte testing [4–6].

Certain criteria for LFIAs including affordable, sensitive, specific, user-friendly, and deliverable to end-users, push researchers to explore new signal tags that have high conversion efficiency and easy readout. Over the years, a variety of signal tags have emerged [7], from traditional colloidal gold nanoparticles (AuNPs) [8, 9], to more sensitive fluorescent particles such as quantum dots (QDs) [10–13], hence the derivative colorimetric and fluorometric LFIA. QDs have advantages in terms of wide spectral coverage from the visible to near-infrared region, narrow and symmetric photoluminescence bands and high fluorescence quantum yields, and are one of the more popular nanomaterials currently utilized within biological applications. We note that the applicability and utility of QDs in LFIA have been demonstrated extensively, and QD-based LFIA shows great competitiveness with promising market shares, particularly due to many commercially available products of water-soluble QDs with functional groups, such as CdSe/ZnS QDs and InP/ZnS QDs modified with carboxyl or amino groups. However, one obstacle to wider implementation of QD-based LFIAs is that their stability and practicability are sometimes hampered by the blinking, photobleaching and oxidative quenching of QD probes [14–17]. Undoubtedly, strict control operations by protection from light exposure that maximally reduce the

photobleaching effect of QD-based LFIAs, cause a serious dilution of user-friendliness. Mostly, the inherent limitation of blinking and photobleaching of QDs results in signal loss, which may increase the false-negative rate. Accordingly, the need remains for an approach that combines the simplicity and easy readout of colorimetric LFIA (such as AuNP-based LFIA) with the improvements in sensitivity of QD-based LFIA—ideally in a format suitable for both laboratory and rapid, on-site applications.

Inspired by the work of Chou et al. [18], in which silver particles are deposited on the QD surface to visualize the distribution of QDs within biological samples under bright field microscopy, we consider that this concept may have good performance in LFIA systems, as silver staining has been proven to improve the sensitivity of the AuNP-based LFIAs (referred to as silver enhancement) [19–21]. In this study, we report the development of a dual signal readout LFIA using silver deposition with QDs, in which QDs are grown into silver clusters to form a visible band under ambient light, while QDs render fluorescent properties under UV light. We sought to develop a simplified dual signal readout LFIA format that would fill in the gaps of QD probes while stressing the advantages of both QDs and silver staining probes. By implementing a silver staining step where silver is deposited directly on the QDs, we improve the suitability and practicability by combining colorimetric and fluorometric bimodal signal readouts, whether precise quantitation in laboratory analysis or semiquantitation in field tests. Furthermore, this approach increases the detection accuracy, by decreasing the false-negative rate, which is induced by the intrinsic defects of QDs (photobleaching and blinking) or by the matrix effect in biological samples of interest.

As a proof of concept, we generated a quantitative and semiquantitative LFIA for the detection of sodium pentachlorophenate (SPC) in chicken samples, a toxic herbicide and bactericide that is banned in animal products by Announcement No.250 of the Ministry of Agriculture and Rural Affairs of the People’s Republic of China [22]. In particular, SPC is frequently found as residue in food of animal origin, such as in chicken muscle, and has become an important object of food safety monitoring. As we have seen, there are some ELISA/AuNP-based LFIA studies or products on the market [23, 24], nevertheless, this is the first report of QD-silver combinations in LFIA for SPC detection. Here, systematic optimizations, including the label strategy of the QD-antibody probe, the concentration of competitive antigens and QD-antibody probes, and the deposition time of silver, were performed. Finally, several metrics, including assay time, assay sensitivity, and assay precision, were used to evaluate the practical value of the developed LFIA, compared with traditional QD-based LFIAs.

2. Materials and methods

2.1. Reagents and materials

Anti-SPC mAb and coating antigen were provided by Kejie Co., Ltd. (Shenzheng, China). Goat-anti-mouse IgG and protein G were obtained from Beijing Solarbio Science & Technology Co., Ltd. (Beijing, China). Carboxylated CdSe/ZnS QDs-525 (8 μM) were purchased from Wuhan Jiayuan Quantum Dot Technology Development Co., Ltd. (Wuhan, China). Silver enhancer A (S5020–100 mL, containing 0.2% silver nitrate), silver enhancer

B (S5145–100 mL, containing 1% hydroquinone), bovine serum albumin (BSA), *N*-(3-(dimethylamino)propyl)-*N*′-ethylcarbodiimide hydrochloride (EDC.HCl), and *N*–hydroxy succinimide (NHS) were obtained from Sigma–Aldrich (St. Louis, MO, USA). All other salts, solvents, and other chemicals of analytical grade came from Aladdin Chemistry Co., Ltd. (Shanghai, China). The elements of the immunochromatographic test strip platform comprising sample pads and nitrocellulose (NC) membranes (pore size = 10 μm) were purchased from Millipore Corp. (Bedford, MA, USA), and absorbent pads and polyvinyl chloride (PVC) cards were purchased from Goldbio Bio. Co. Ltd. (Shanghai, China).

Buffers for immune probe synthesis, sample extraction and sample analysis, such as phosphate buffered saline (PBS, 10 mM, pH 7.4), citric acid solution (100 mM) and PBST (10 mM PBS containing 0.05% Tween-20, pH 7.4) were provided by Beijing Solarbio Science & Technology Co., Ltd. (Beijing, China). Carbonate buffer saline (CBS, 50 mM, pH 9.6) was prepared for ELISA, and PBS solution containing 0.02% NaN3, 2% BSA, 2.5% sucrose and 0.25% Tween-20 was used to block the sample pad.

2.2. Immune probe synthesis (QD-protein G)

We prepared an immune probe following protocols from references [25, 26] and the manufacturers using EDC/NHS coupling. The surfaces of commercially available QDs are functionalized with polyacrylic acid to have a 300~500 -COOH density per QD, as described by the manufacturers. The carboxylated QDs (20 μL, 8 μM) were activated by adding 8 μL of EDC (4 mg/mL in 10 mM PBS, an excess of EDC was used in a ratio of 1000 mol of EDC per mol of carboxylated QDs) and 6.8 μL of NHS (4 mg/mL in 10 mM PBS) followed by 70 μL of PBS buffer to a volume of 100 μL. The mixtures were gently stirred at room temperature (RT) for 30 min, after which protein G (1 mg/mL in 10 mM PBS) was added (the molar ratios of QDs:protein G between 1:1 up to 1:5 were optimized). The reaction was then incubated at RT for 2 h on a rotating wheel in the dark. Then, the mixtures were stabilized by adding 10 μL of BSA (100 mg/mL) with stirring for 1 h. The solution was centrifuged at 7000 ×g for 3 min to remove aggregated QDs, and the supernatant was collected for further study.

The emission spectra of QD-protein G probes were acquired to evaluate their optical properties relative to free QDs using a Spark 10M multimode microplate reader (Tecan, Switzerland). Then, the binding efficiency of the labeled QD-protein G conjugates was evaluated by the LFIA.

2.3. LFIA strip fabrication

The LFIA test strip was assembled by adhering the sample pad, nitrocellulose (NC) membrane and absorbent pad (high density cellulose) onto a polyvinyl chloride card. The sample pad (cellulose or glass fiber) was first cut to a size of 2 × 30 cm and then modified by soaking in a blocking solution containing 0.02% NaN_3, 2% BSA, 2.5% sucrose and 0.25% Tween-20 and dried at 37°C for 2 h. Coating antigen (0.5 mg/mL) and goat anti-mouse IgG (0.35 mg/mL) were spotted onto NC membrane (3 × 30 cm) to form the test line (T) and control line (C), respectively, at a rate of 1 μL/cm using the BioDot XYZ 3050 Dispensing Platform. The NC membrane was then dried at 37°C for 30 min. Finally, the test

strip was assembled by sticking the absorbent pad, NC membrane, and sample pad onto a backing card, and the sample pads and absorbent pads were attached to both ends of the NC membrane with 2 mm overlap. The as-prepared card was cut into individual strips with a width of 4.0 mm and was fitted into plastic cassettes for further use.

2.4. Assay protocols

In a conventional QD-based LFIA analysis the following experimental procedure was performed. First, 50 μL of standards (or sample extracts) were mixed with 50 μL of detection probes (10 mM PBS buffer containing 0.5 μL of QD-protein G conjugates and 4 μL of free anti-SPC mAb (0.3 mg/mL)). In this step, the analytes in samples efficiently combined with the unoccupied antibodies. After incubation at room temperature (RT) for 5 min, the solution was applied directly to the test strip by adding the solutions onto the sample pad or by inserting the strip into the solutions. After 12 min, fluorescence photographs of the test strips were taken by a smartphone (iPhone XR) using the rear-facing camera under UV light (365−400 nm UV irradiation), and the fluorescence intensities of the T line were recorded by using a portable fluorescence strip reader.

In the silver deposition step, the test strip was incubated at 37°C for 10 min for better absorption of silver solution. Then, the strip was inserted into a mixed solution of silver enhancers A (50 μL) and B (50 μL) for 5 min. Finally, a photograph of the test strip was taken by the same smartphone under natural light.

2.5. Signal processing

Assay results were analyzed as qualitative/semiquantitative and quantitative detection by visual reading and quantitative calculation. Specifically, for qualitative/semiquantitative detection, the visual reading produced by the lowest concentration of SPC that can be easily discriminated from the zero signal, was set as the visual limit of detection (V-LOD).

For quantitative detection, the color intensity was collected by a portable fluorescence strip reader to construct a calibration curve between the SPC concentration and color intensity of the T line. The calibration curve was plotted in Origin 8.5 software (OriginLab, MA, USA) with a four-parameter logistic equation for line fitting:

$$Y = A_2 + \left(A_1 - A_2\right) / \left[1 + \left(X / X_0\right)^P\right.$$

where Y represents the fluorescence intensity of the T line, X is the concentration of SPC, A_1 and A_2 are the fluorescence intensities at the saturated analyte concentration and zero analyte concentration, X_0 is the concentration of SPC at 50% of the binding rate (EC_{50}) and P is the slope at the EC_{50} point. As a quantitative (for LFIA—instrumental) LOD, the SPC concentration causing 90% inhibition of the signal (IC_{90}) was considered. The lower and upper limits of the working range were estimated as the SPC concentrations corresponding to 80% (IC_{80}) and 20% (IC_{20}) inhibition of the signal, respectively [27].

2.6. Analysis of chicken samples

Chicken samples purchased from local supermarkets, were used to test the recovery. Five grams of SPC-free chicken muscle homogenate certified by HPLC−MS/MS was spiked with SPC to obtain tissue levels of 50 and 100 μg/kg, respectively. The samples were mixed vigorously with 0.5 mL of ethyl acetate and 6.0 mL of hexane for 5 min. The mixture was centrifuged for 5 min at 4500× g at room temperature. Six milliliters of the supernatants were dried and redissolved in 400 μL PBS (0.01 M, pH 7.4). Finally, the solution was diluted 5-fold with running buffer (0.01 M PBS containing 0.1% Tween-20, pH 7.4) for LFIA detection. Reference methods including ELISA and HPLC−MS/MS, are provided in the supporting information.

3. Results and discussion

3.1. Strategy of the QD-silver LFIA

Our approach makes use of silver deposition coupled with QDs as dual signal outputs in a lateral flow immunoassay—which we term QD-silver LFIA—that can detect small molecular compounds in both colorimetric and fluorometric modes. Our objective is to exploit the ability of silver deposition on QDs to overshadow the weakness of traditional QD-based LFIA, as to enhance the practicability of LFIA.

In the first step of the QD-silver LFIA (Fig. 1), a competitive immunoassay takes place on the T line, where the analyte in the sample (here represented as SPC) and the antigen immobilized on the T line compete for the limited binding sites of the QD-labeled antibodies. Thanks to the fluorescence characteristics of QDs, the concentration of SPC is inversely proportional to the fluorescence intensity of QDs, as visualized under UV light or recorded by a fluorescence reader. In the second step, the silver particles are deposited on the QD surface by a reduction process, where the transfer of electrons from the reducing agent (e.g., hydroquinone) through the nanostructure to adhering silver ions reduces the latter to metallic silver. In addition, the deposited silver atoms on the QD surface assume the same catalytic role as the original nanostructure by recruiting additional silver atoms onto the surface, finally effectively amplifying the silver layer size until visible under magnification. Thus, the signals of the T line are directly visualized under natural light, combining the high sensitivity of fluorometric mode with the easy readout of colorimetric mode in one LFIA. More importantly, silver deposition overcomes the potential false-negative results of QD-based LFIAs, which are induced by the intrinsic defects of QDs, such as photobleaching, blinking and oxidative quenching. That is, a double-checked operation is performed within 12–27 min, rendering the LFIA more accurate and more sensitive, as well as more user friendly.

3.2. Characterization of the immune probe

To generate a specific immune probe, the key reagent of our assay, we first coupled the specific antibody to QDs. EDC/NHS crosslinking has been proven to form robust amide crosslinks between carboxylates (-COOH) and primary amines ($-NH_2$) [28, 29]. In our original concept, we tried to use the anti-SPC monoclonal antibody (SPCmAb) to directly immobilize on carboxylated QDs. Unfortunately, the QD-SPCmAb probe had weak

recognition even at high coating antigen concentrations (Fig. 2a). Meanwhile, the AuNP-SPCmAb conjugates using the classic physical adsorption method, showed an obvious red band at lower coating antigen concentrations (Fig. 2a). We deduced that the covalent coupling method had a negative effect on the activity of the SPCmAb, as the free -NH_2 always comes from lysines in antibodies, which are sometimes the key amino acids in the antibody-antigen binding site. In this case, modification of the lysine would decrease the capability of antigen binding, resulting in low sensitivity of LFIA.

For maximal binding efficiency, it is necessary to achieve immobilization of antibodies while ensuring orientation of solution-facing antigen binding regions. Utilizing anti-species antibody or protein G/A, which specifically binds to the Fc region of antibody (Ab1), could support Ab1 with a high degree of controlled orientation and a high antigen-binding capacity [30–32]. In our study, protein G was first immobilized on QDs using EDC/NHS crosslinking. Free SPCmAb was mixed with the QD-protein G conjugates to form the specific immune probe. The QD-protein G conjugates were characterized to evaluate the possible effect of the coupling process on the luminescence emission of the QDs labeled with the antibody. As shown in Fig. 2b, both QD-protein G conjugates and free QDs present intense fluorescence at an emission wavelength of 522 nm. Moreover, in Fig. 2a, a strong fluorescence band is observed at the test zone of the strip, showing the high activity of both protein G and SPCmAb after bioconjugation. Further experiments demonstrated many advantages associated with indirect labeling.

3.3. Nonspecific adsorption of the proposed LFIA

Our concept is to explore the silver deposition on the QD-based immune probe that improves the performance of the fluorescent LFIA. In contrast to the work of Chou et al. [18], in which nonprotein-modified QDs were proven to attract silver ions to deposit on their surface in paraffin-embedded biological tissues, we tried to evaluate the feasibility of this concept in protein labeled QDs and their function in NC membrane substrates, since silver deposition has been extensively used in protein staining [33, 34]. Confirming the specific silver deposition signals that are induced by the QDs, but not by the antibody modified on the QD surface, is important to the developed LFIA. In addition, the silver deposition efficiency on the QD surface in the lateral flow system needs to be considered. Here, control groups containing only free SPCmAb or pure running solution were operated according to the strip assay protocol in the chapter “Assay protocols”, by detecting the color intensity of T lines after silver deposition. From the data in Fig. 3, the control groups have no gray bands of T lines, which indicates the immobilized coating antigen in the T line (BSA as carrier protein) or the antigen-antibody complex formed in the T line has low silver deposition efficiency in such deposition time (5 min) and protein concentration (0.3 mg/mL), while the QD-protein G & SPCmAb group has visible gray bands both in the T line and C line.

3.4. Assay optimization

A series of optimization experiments were performed to achieve better sensitivity and to characterize the LFIA for further applications. In our assay, the signal response was inversely proportional to the dose of analyte, described as a competitive immunoassay. Bringing down the dose of antibodies and/or competitors as much as possible, was qualified

as practical to increase the sensitivity of competitive immunoassay, but only if a tolerably detectable signal was obtained [35, 36]. That is, the volume of immune probe (QD-protein G and SPCmAb) and concentration of competitive antigen coated on the T line are the key parameters to be optimized.

In our system, we utilized a fixed coating antigen concentration to run the single-factor experimental analysis. The ratio of the signal (fluorescence intensity of the T line recorded in the absence and presence of SPC in the sample; FL_0/FL) was chosen as the evaluation criterion. The concentration of SPC was set at 10 ng/mL, and QD-protein G volumes from 0.25 μL to 2.0 μL were examined. As shown in Fig. S1, the highest signal ratio was obtained at a QD-protein G volume of 0.5 μL, and a sufficiently strong visual signal was observed, which showed the strongest competitive capability of the analytes against the immobilized antigens.

Doses of SPCmAb ranging from 2 μL to 8 μL (0.3 mg/mL) were optimized. A lower SPCmAb dosage (2 μL) did not show a clear test line at the SPC free concentration, while SPCmAb dosages over 4 μL had lower sensitivity because more SPC was needed to compete with the antigen for the limit binding sites of SPCmAb (Fig. S2).

Additionally, the deposition time of silver was also investigated. Figure S3 shows the gray band of the silver stains formed after 3 min of development. The amount of deposited silver at the T line increased with increasing deposition time. However, a longer deposition time of the silver enhancer solution produced a higher background. With a deposition time of 5 min, the signal-to-noise ratio was maximal.

Other experimental conditions such as the incubation time of the sample and detection probe, fluorescence readout time, concentration of Tween-20 in running buffer, pH value of running buffer, and volume of silver solution, were also optimized, and all final experimental conditions selected are summarized in Table 1.

3.5. Analytical performance characteristics

Our assay permitted the detection of SPC from a 50 μL sample with concentrations ranging over two orders of magnitude with a visual limit of detection (V-LOD) of 10 ng/mL under fluorometric mode (Fig. 4a). For quantitative analysis, the corresponding inhibition curve was fitted using a four-parameter equation, and a linear relationship was achieved ranging from 4.4 to 59.2 ng/mL (IC_{20}−IC_{80}) enabling SPC trace determination in aqueous media (Fig. 4c). The detection limit (LOD), calculated as IC_{10} in the inhibition curve, was 1.45 ng/mL of SPC. As we can see, it is not easy to capture the fluorescence colors of the T line at SPC concentrations over 25 ng/mL, but a clear band was observed at SPC concentrations of 100 ng/mL after silver deposition (Fig. 4a & 4b), which showed 4-fold signal enhancement. Meanwhile, the gray levels of the lines were well proportional to the dose of captured fluorescent probes. Deposition of silver on QDs after usual strip development and QD focalization in the reactive zone, led to the achievement of improved detectability in terms of the increment of the dimension of each single nanoparticle [37], and more intensive color contrast from green/black contrast (fluorometric mode) to black/white contrast (colorimetric mode). This creates possibilities for sensitivity improvement

by reducing immunoreagent amounts, such as the amount of labeled antibody probes or of competitive antigens, and thus favoring competition. This strategy has been studied in many reports and showed dependable results for sensitivity improvement for competitive immunoassays [36, 38, 39]. By using this strategy, the V-LOD of the strips after silver deposition was 4 ng/mL, which showed a 2.5-fold improvement in the detection limit (Fig. S4). It should be noted, however, that over concern with the high sensitivity of the colorimetric mode can damage the stability of the fluorometric assay, since the aim of silver deposition is to overcome the signal loss of QD probes.

We tested the false-negative rate by using simulated signal loss of QD probes under abnormal operating conditions, such as long exposure to natural light, whether in long-term storage or assay operation, which is an inevitable problem that occurs in grassroots users. SPC (15 ng/mL) was set as the positive level in the standard LFIA judged by visual readout. Ten aqueous media samples spiked with 15 ng/mL SPC were used to run the assay under a QD probe exposed to natural light for 30 min. As shown in Table 2 and Fig. S5, all LFIA results were negative under typical QD strip development, but were positive after silver deposition. Actually, the signal loss of QD probe caused a false dose–response relation, because the differences in signal fading in the T lines were small before and after adding the analyte. However, the signal enhancement of silver deposition contributed to the sensitive dose response, and the colorimetric signal intensity derived from the amount of silver-QD complex, which really showed the true antibody-antigen combination dose, thus caused more accurate detection results. It should be stressed here that some additional complexity is incurred by the use of a silver deposition step, but this is more than offset by the greater benefits in assay performance achieved.

3.6. Application to chicken sample analysis

The usefulness of the developed QD-silver LFIA to determine SPC contents in chicken matrices was initially studied using spiked samples. Chicken breast samples collected from a local market were confirmed to be SPC free by the reference HPLC−MS/MS method. Thereafter, blank chicken samples were spiked with SPC at concentrations of 50 μg/kg and 100 μg/kg, respectively. The accuracy of the developed LFIA was evaluated by testing spiked samples. All artificially contaminated samples were determined to be positive by the developed LFIA (positive was defined as visual reading of T lines that can be easily discriminated from the zero signal) in both colorimetric and fluorometric modes (Fig. S6). Quantitative results showed a recovery range of 94.0%−97.6% (Table 3), and all ELISA and HPLC−MS/MS results were very close to the spiked levels, demonstrating the high correlation between visually assessed LFIA and reference methods. For real sample analysis, a declining band was found by using a naturally contaminated chicken sample at a detectable level of 22.5 μg/kg (P49527, provided by Beijing Puyan Standard Technology Co., LTD), and all recovery data fell into the range of 95.6–100%.

4. Conclusions

A compelling challenge and a constant pursuit in LFIA is to improve the assay performance, such as sensitivity and accuracy, but without compromising the simplicity and practicality.

We have shown that silver deposition on quantum dots is well adapted for developing dual signal readout LFIAs, which brings benefits to signal enhancement and accuracy improvement relative to those in conventional quantum dot-based LFIAs.

The signal enhancement is the result of an amplification step that causes a small amount of silver to grow on QD surface after usual strip development; therefore, a more intense color contrast is formed, leading to improved detectability. Apart from that, what is more important, the colorimetric signal generated from silver deposition could reflect a true quantitative relation between the analyte and its specific immune probe, which sometimes produces false results in QD-based LFIA due in part to the inherent defects of QD probes. As a result, more accurate detection is available with only a simple silver staining step.

This integrated approach actually does little to increase the complexity, detection time and even the cost of the assay, since the silver deposition step is finished by a direct insertion of the strip into the staining solution within 5 min, and the staining solutions containing silver salt (nitrate or acetate) with a reducing agent (hydroquinone) are available in many commercial producers and are very inexpensive. In this case, the integrated LFIA enhances the user-friendliness, particularly to those who have no professional skills in running an immunoassay. The application of this LFIA was evaluated for sodium pentachlorophenate (SPC) detection in chicken products, which is urgently needed by chicken breeders and chicken product producers, because SPC is one of the key monitoring targets in food of animal origin in China. We hope the developed LFIA could be a powerful tool for the field of rapid testing and diagnostics.

Supplementary Material

Refer to Web version on PubMed Central for supplementary material.

Funding:

This work was supported by the National Natural Science Foundation of China (32272591, 32072311), the National Key R&D Program of China (2019YFC1605902), the National Institute of Environmental Health Science Superfund Research Program (P42 ES004699), and the RIVER Award (R35 ES030443-01).

References

[1]. Posthuma-Trumpie GA, Korf J, Amerongen AV, Lateral flow (immuno)assay: its strengths, weaknesses, opportunities and threats. A literature survey, Anal. Bioanal. Chem 393 (2009) 569–582, 10.1007/s00216-008-2287-2. [PubMed: 18696055]

[2]. Khlebtsov B, Khlebtsov N, Surface-Enhanced Raman Scattering-Based Lateral-Flow Immunoassay, Nanomaterials 10 (2020) 2228, 10.3390/nano10112228. [PubMed: 33182579]

[3]. Di Nardo F, Chiarello M, Cavalera S, Baggiani C, Anfossi L, Ten Years of Lateral Flow Immunoassay Technique Applications: Trends, Challenges and Future Perspectives, Sensors 21 (2021) 5185, 10.3390/s21155185. [PubMed: 34372422]

[4]. Du Y, Pothukuchy A, Gollihar JD, Nourani A, Li B, Ellingtonet AD, Coupling Sensitive Nucleic Acid Amplification with Commercial Pregnancy Test Strips, Angew. Chem. Int. Ed 56 (2017) 992–996, 10.1002/anie.201609108.

[5]. Prakashan D, Shrikrishna NS, Byakodi M, Nagamani K, Gandhi S, Gold nanoparticle conjugate-based lateral flow immunoassay (LFIA) for rapid detection of RBD antigen of SARS-CoV-2

in clinical samples using a smartphone-based application, J. Med. Virol (2022) e28416, 10.1002/jmv.28416.

[6]. Prainito CD, Eshun G, Osonga FJ, Isika D, Centeno C, Sadik OA, Colorimetric Detection of the SARS-CoV-2 Virus (COVID-19) in Artificial Saliva Using Polydiacetylene Paper Strips, Biosensors 12 (2022) 804, 10.3390/bios12100804. [PubMed: 36290942]

[7]. Byakodi M, Shrikrishna NS, Sharma R, Bhansali S, Mishra Y, Kaushik A, Gandhi S, Emerging 0D, 1D, 2D, and 3D nanostructures for efficient point-of-care biosensing, Biosens. Bioelectron 12 (2022) 100284, 10.1016/j.biosx.2022.100284.

[8]. Gandhi S, Caplash N, Sharma P, Suri CR, Strip-based immunochromatographic assay using specific egg yolk antibodies for rapid detection of morphine in urine samples, Biosens. Bioelectron 25 (2009) 502–505, 10.1016/j.bios.2009.07.018. [PubMed: 19699078]

[9]. Roberts A, Prakashan D, Dhanze H, Gandham RK, Gandhi S, Sharma GT, Immuno-chromatic probe based lateral flow assay for point-of-care detection of Japanese encephalitis virus NS1 protein biomarker in clinical samples using a smartphone-based approach, Nanoscale Adv. 4 (2022) 3966, 10.1039/D2NA00463A. [PubMed: 36133331]

[10]. Sun J, Li Y, Pi F, Ji J, Zhang Y, Sun X, Using fluorescence immunochromatographic test strips based on quantum dots for the rapid and sensitive determination of microcystin-LR. Anal. Bioanal. Chem 409 (2017) 2213–2220, 10.1007/s00216-016-0166-9. [PubMed: 28108754]

[11]. Liu J, Wang B, Huang H, Jian D, Lu Y, Shan Y, Wang S, Liu F, Quantitative ciprofloxacin on-site rapid detections using quantum dot microsphere based immunochromatographic test strips, Food Chem. 335 (2021) 127596, 10.1016/j.foodchem.2020.127596. [PubMed: 32745840]

[12]. Wang C, Hou F, Ma Y, Simultaneous quantitative detection of multiple tumor markers with a rapid and sensitive multicolor quantum dots-based immunochromatographic test strip, Biosens. Bioelectron 68 (2015) 156–162, 10.1016/j.bios.2014.12.051. [PubMed: 25562743]

[13]. Liu C, Zhao J, Zhang R, Zhang Z, Xu J, Sun A, Chen J, Shi X, Development and application of fluorescence sensor and test strip based on molecularly imprinted quantum dots for the selective and sensitive detection of propanil in fish and seawater samples. J. Hazard. Mater 389 (2020) 121884, 10.1016/j.jhazmat.2019.121884. [PubMed: 31879102]

[14]. Schwartz O, Tenne R, Levitt JM, Deutsch Z, Itzhakov S, Oron D, Colloidal Quantum Dots as Saturable Fluorophores, ACS Nano 6 (2012) 8778–8782, 10.1021/nn302551v. [PubMed: 22992215]

[15]. Wichner SM, Mann VR, Powers AS, Segal MA, Mir M, Bandaria J, DeWitt MA, Darzacq X, Yildiz A, Cohen BE, Covalent Protein Labeling and Improved Single Molecule Optical Properties of Aqueous CdSe/CdS Quantum Dots, ACS Nano 11 (2017) 6773–6781, 10.1021/acsnano.7b01470. [PubMed: 28618223]

[16]. Mancini MC, Kairdolf BA, Smith AM, Nie S, Oxidative Quenching and Degradation of Polymer-Encapsulated Quantum Dots: New Insights into the Long-Term Fate and Toxicity of Nanocrystals in Vivo, J. Am. Chem. Soc 130 (2008) 10836–10837, 10.1021/ja8040477. [PubMed: 18652463]

[17]. Yeh CW, Chen GH, Ho SJ, Chen HS, Inhibiting the Surface Oxidation of Low-Cadmim-Content ZnS:(Cd,Se) Quantum Dots for Enhancing Application Reliability, ACS Appl. Nano Mater 2 (2019) 5290–5301, 10.1021/acsanm.9b01213.

[18]. Chou LYT, Fischer HC, Perrault SD, Chan WCW, Visualizing Quantum Dots in Biological Samples Using Silver Staining, Anal. Chem 81 (2009) 4560–4565, 10.1021/ac900344a. [PubMed: 19408951]

[19]. Yang W, Li X, Liu G, Zhang B, Zhang Y, Kong T, Tang J, Li D, Wang Z, A colloidal gold probe-based silver enhancement immunochromatographic assay for the rapid detection of abrin-a, Biosens. Bioelectron 26 (2011) 3710–3713, 10.1016/j.bios.2011.02.016. [PubMed: 21377861]

[20]. Moumita M, Shankar KM, Abhiman PB, Shamasundar BA Development of a sandwich vertical flow immunogold assay for rapid detection of oxytetracycline residue in fish tissues, Food Chem. 270 (2019) 585–592, 10.1016/j.foodchem.2018.07.124. [PubMed: 30174090]

[21]. Deng Y, Jiang H, Li X, Lv X, Recent advances in sensitivity enhancement for lateral flow assay, Microchim. Acta 188 (2021) 379, 10.1007/s00604-021-05037-z.

[22]. Announcement No.250 of the Ministry of Agriculture and Rural Affairs of the People's Republic of China (2020) http://www.moa.gov.cn/gk/tzgg_1/gg/202001/t20200106_6334375.htm.

[23]. Liu H, Feng C, Jia F, Feng J, Peng G, Zhang Y, Study on the production of pentachlorophenoi-Na monoclonal antibodies and its enzyme linked immunosorbent assay kit for rapid detection, Sci. Technol. Food Industry 21 (2015) 307, 10.13386/j.issn1002-0306.2015.21.055.

[24]. Luo XQ, Han S, Lv YQ, Liu Y, Cao DS, Wang JX, Study on gold immunochromatography assay for rapid detection of pentachlorophenol-Na, Journal of Anhui Agricultural Sciences 44 (2016) 55–57, 10.13989/j.cnki.0517-6611.2016.25.020.

[25]. Dong T, Yangxiao K, Zhao K, Deng A, Li J, Signal Amplification Strategy for Highly Sensitive Detecting Brombuterol with Electrochemiluminescent Immunoassay by Using CdSe QDs as Label and Gold Nanoparticle as Substrate, Electroanalysis 28 (2016) 1847–1855, 10.1002/elan.201600332.

[26]. Liu J, Ji D, Meng H, Zhang L, Wang J, Huang Z, Chen J, Li J, Li Z, A portable fluorescence biosensor for rapid and sensitive glutathione detection by using quantum dots-based lateral flow test strip, Sensor Actuat. B-Chem 262 (2018) 486–492, 10.1016/j.snb.2018.02.040.

[27]. Hendrickson OD, Zvereva EA, Vostrikova NL, Chernukha IM, Dzantiev BB, Zherdev AV, Lateral flow immunoassay for sensitive detection of undeclared chicken meat in meat products, Food Chem. 344 (2020) 128598, 10.1016/j.foodchem.2020.128598.

[28]. Staros JV, Wright RW, Swingle DM Enhancement by N-hydroxysulfosuccinimide of water-soluble carbodiimide-mediated coupling reactions, Anal. Biochem 156 (1986) 220–222, 10.1016/0003-2697(86)90176-4. [PubMed: 3740412]

[29]. Grabarek Z, Gergely J Zero-length crosslinking procedure with the use of active esters, Anal. Biochem 185 (1990) 131–135, 10.1016/0003-2697(90)90267-D. [PubMed: 2344038]

[30]. Li G, Xu L, Wu W, Wang D, Jiang J, Chen X, Zhang W, Poapolathep S, Poapolathep A, Zhang Z, Zhang Q, Li P, On-Site Ultrasensitive Detection Paper for Multiclass Chemical Contaminants via Universal Bridge-Antibody Labeling: Mycotoxin and Illegal Additives in Milk as an Example, Anal. Chem 91 (2019) 1968–1973, 10.1021/acs.analchem.8b04290. [PubMed: 30509070]

[31]. Zha C, An X, Zhang J, Lin W, Zhang Q, Yang Q, Li F, Sun X, Guo Y, Indirect signal amplification strategy with a universal probe-based lateral flow immunoassay for the rapid quantitative detection of fumonisin B1, Anal. Methods 14 (2022) 708–716, 10.1039/d1ay01625c. [PubMed: 35103722]

[32]. Clarizia L, Sok D, Wei M, Mead J, Barry C, McDonald M, Antibody orientation enhanced by selective polymer-protein noncovalent interactions, Anal. Bioanal. Chem 393 (2009) 1531–1538, 10.1007/s00216-008-2567-x. [PubMed: 19104778]

[33]. Sorensen B, Hojrup P, Ostergard E, Jorgensen CS, Enghild J, Ryder LR, Houen G, Silver staining of proteins on electroblotting membranes and intensification of silver staining of proteins separated by polyacrylamide gel electrophoresis, Anal. Biochem 304 (2002) 33–41, 10.1006/abio.2001.5604. [PubMed: 11969186]

[34]. Grimelius L, Silver stains demonstrating neuroendocrine cells, Biotech. Histochem 79 (2004) 37–44, 10.1080/10520290410001715264. [PubMed: 15223752]

[35]. Byzova NA, Zvereva EA, Zherdev AV, Eremin SA, Sveshnikov PG, Dzantiev BB, Pretreatment-free Immunochromatographic assay for the detection of streptomycin and its application to the control of milk and dairy products, Anal. Chim. Acta 701 (2011) 209–217, 10.1016/j.aca.2011.06.001. [PubMed: 21801890]

[36]. Anfossi L, Di Nardo F, Giovannoli C, Passini C, Baggiani C Increased sensitivity of lateral flow immunoassay for ochratoxin A through silver enhancement, Anal. Bioanal. Chem 405 (2013) 9859–9867, 10.1007/s00216-013-7428-6. [PubMed: 24162821]

[37]. Yu Q, Li H, Li C, Zhang S, Sheng J, Wang Z, Gold nanoparticles-based lateral flow immunoassay with silver staining for simultaneous detection of fumonisin B1 and deoxynivalenol, Food control 54 (2015) 347–352, 10.1016/j.foodcont.2015.02.019.

[38]. Liu B, Tsao Z, Wang J, Yu F, Development of a monoclonal antibody against ochratoxin A and its application in enzyme-linked immunosorbent assay and gold nanoparticle immunochromatographic strip, Anal. Chem 80 (2008) 7029–7035, 10.1021/ac800951p. [PubMed: 18698802]

[39]. Liu Y, Xie R, Guo Y, Zhu G, Tang F, Comparison of homologous and heterologous formats in nanocolloidal gold-based immunoassays for parathion residue determination, J. Environm. Sci. Health B 47 (2012) 475–483, 10.1080/03601234.2012.663613.

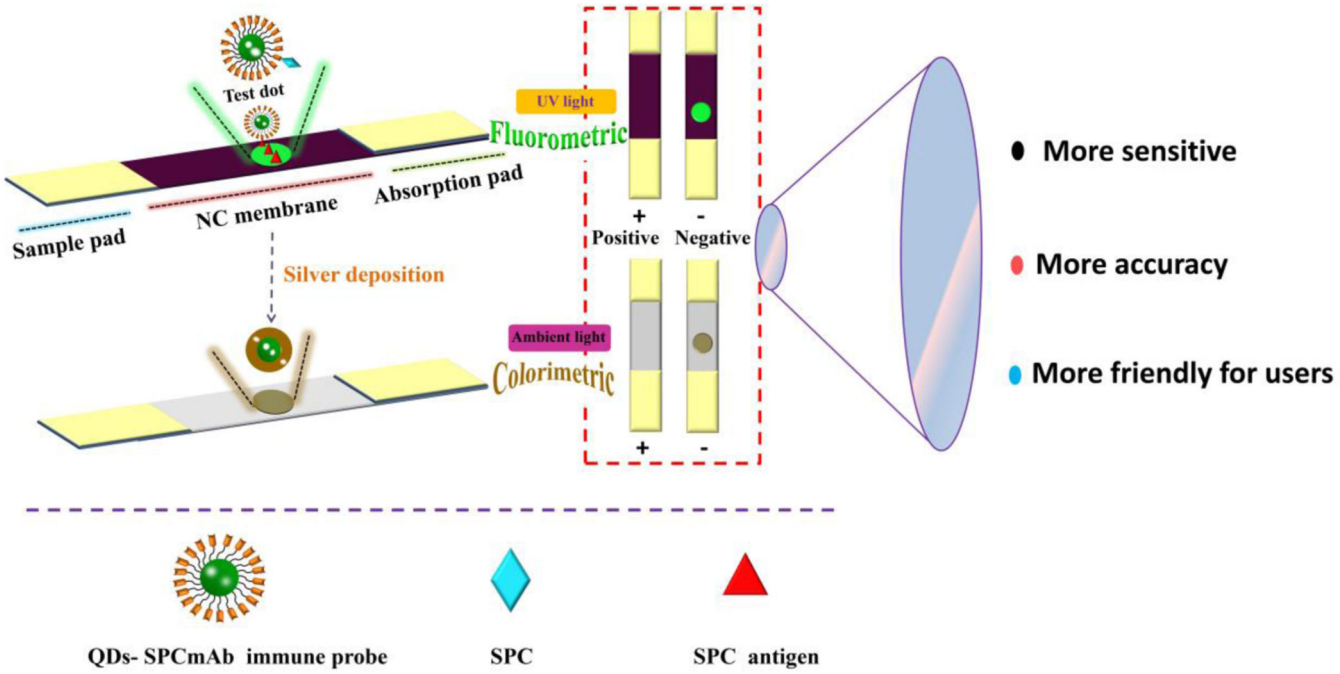

Fig. 1.

Schematic of the QD-Silver LFIA: (top) QD-SPCmAb conjugates are used to competitively capture the SPC in samples and antigen immobilized on the test zone. Semiquantitative results are visualized with UV light to excite the luminescence of QDs. (bottom) Silver deposits on the QDs, which are captured on the test zone, to form a magnified QD-silver complex, enabling direct visualization under natural light. Note: The antibody/protein labeled in the immune probe and the numbers of lines/dots in the test zone can vary.

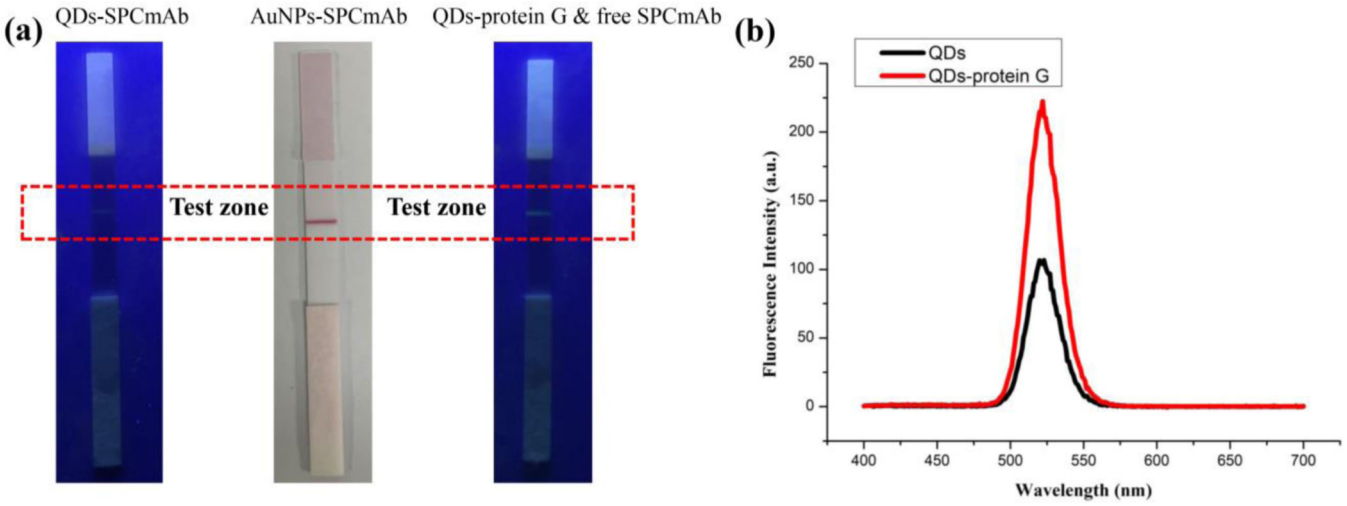

Fig. 2.

(a) Visualization of binding efficiency for different labeled immune probes. The test zone was coated with SPC antigen at concentration of a 2 mg/mL for the QD-SPCmAb probe, 0.5 mg/mL for the AuNP-SPCmAb probe and the QD-protein G & free SPCmAb probe, respectively. (b) Fluorescence spectrum of QDs and QD-conjugated protein G (QD-protein G). The concentrations of QDs and QD-protein G conjugates were 0.26 μM and 0.45 μM, respectively.

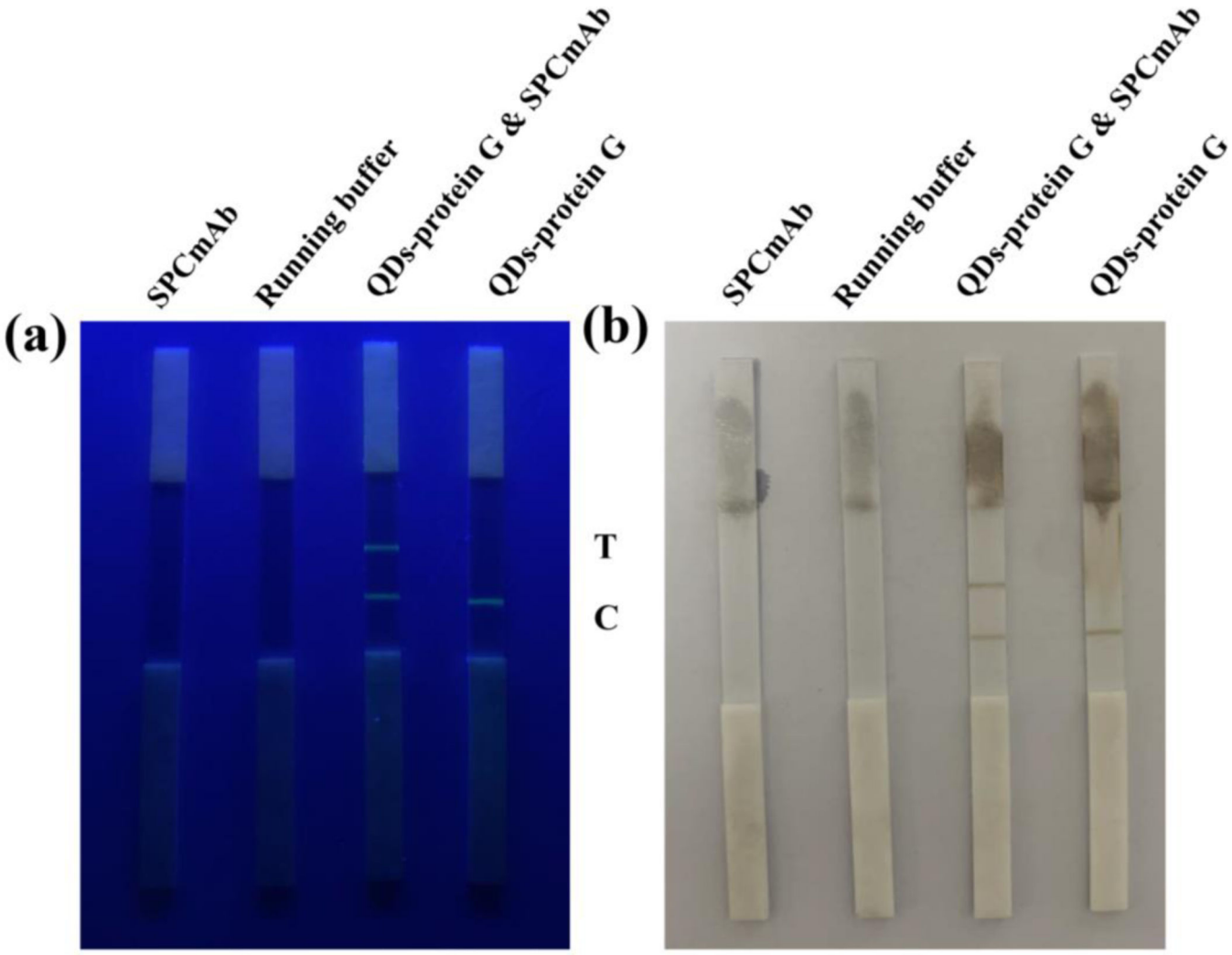

Fig. 3.

Visualization of nonspecific adsorption for different immune probe groups. (a) Fluorometric photo after usual QD-based LFIA development; (b) Colorimetric photo after silver deposition development. The T line was coated with SPC antigen at a concentration of 0.5 mg/mL, and the C line was coated with goat anti-mouse IgG at a concentration of 0.5 mg/mL.

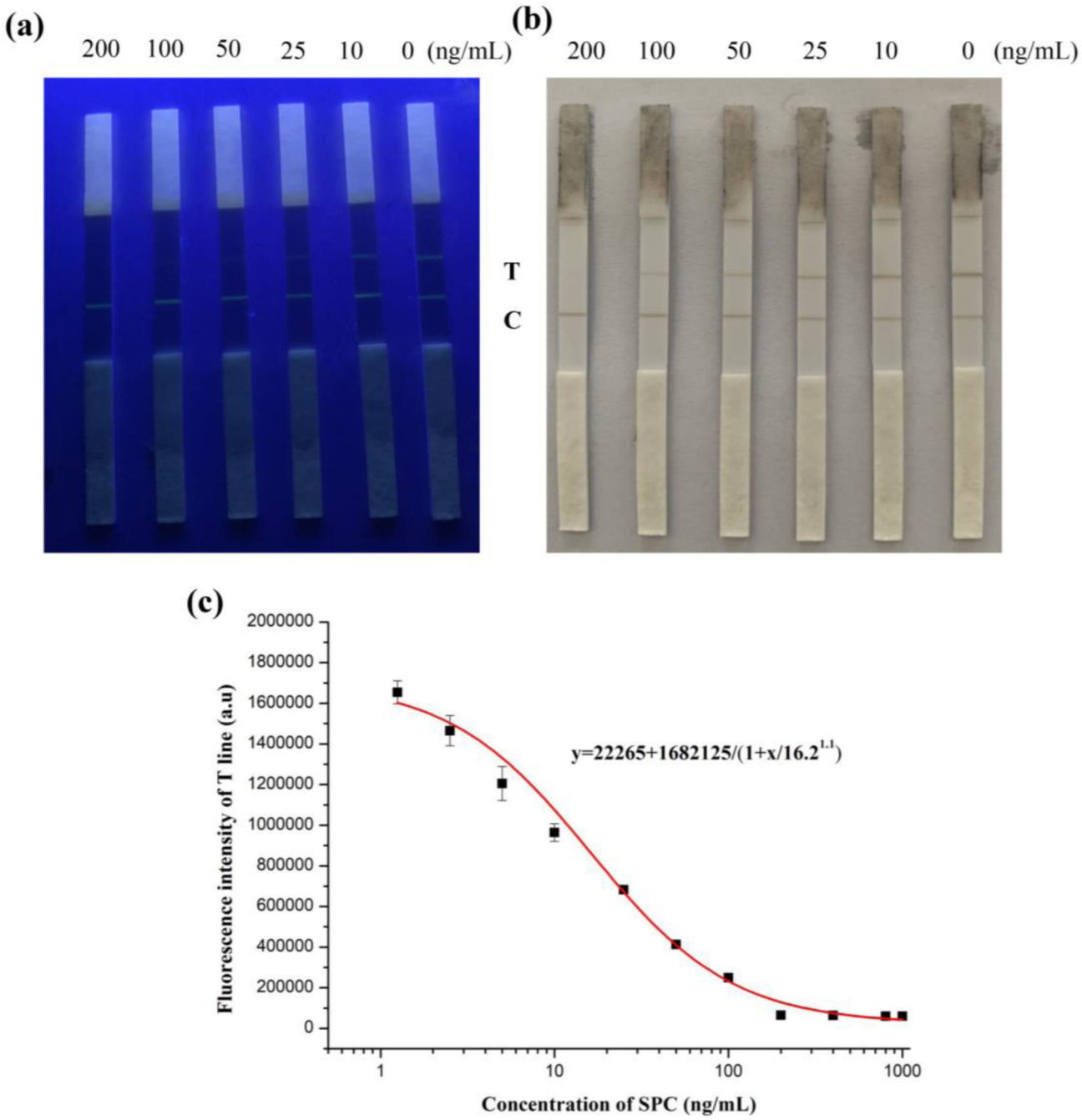

Fig. 4.

Detection limit of the proposed QD-silver LFIA. SPC standard solutions at concentrations of 0, 10, 25, 50, 100 and 200 ng/mL were assayed. (a) Fluorometric signal of typical QD strip development. (b) Colorimetric signal under natural light by application of silver deposition. (c) Quantification standard curve of raw data presented in fluorometric results.

Table 1

Optimized experimental conditions of the proposed QD-silver LFIA.

Step/condition	Optimized value
Incubation time of sample and detection probe	5 min
Fluorescent readout time	12 min
Concentration of Tween-20 in running buffer	0.1%
pH value of running buffer	7.4
Volume of silver solution	100 μL

Table 2

Detection results of the proposed QD-silver LFIA for SPC at positive level under simulated abnormal operating conditions.

Sample No.	Readout results		
	Typical QD-based LFIA (Fluorometric mode)	Silver deposition LFIA (Colorimetric mode)	HPLC−MS/MS (ng/mL)
1	−	+	15.1
2	−	+	15.0
3	−	+	14.9
4	−	+	14.9
5	−	+	14.9
6	−	+	14.9
7	−	+	15.1
8	−	+	15.0
9	−	+	15.3
10	−	+	15.1

“−” negative, defined as the color intensity of T line is equal to that of zero signal

“+” positive, defined as the color intensity of T line is weaker than that of zero signal

Table 3

Comparison of the proposed QD-silver LFIA, ELISA and HPLC−MS/MS in analysis of chicken samples spiked/naturally contaminated by SPC.

Type of sample	SPC concentration (μg/kg)	QD-silver LFIA			ELISA		HPLC−MS/MS	
		Visual detection[a]	Mean[b] (μg/kg)	Recovery (%)	Mean (μg/kg)	Recovery (%)	Mean (μg/kg)	Recovery (%)
Spiked sample 1	0	−	0	NA[c]	0	NA	0	NA
Spiked sample 2	50	+	48.8	97.6	49.2	98.4	50.5	101
Spiked sample 3	100	+	94.0	94.0	96.5	96.5	103.0	103
Natural sample	22.5	+	21.5	95.6	22.0	97.8	22.5	100

[a]Visual assessment of the test line; (−) negative result (defined as the color intensity of T line is equal to that of zero signal); (+) positive result (defined as the color intensity of T line is weaker than that of zero signal);

[b]Quantitative assessment by using a four-parameter equation from fluorometric mode

[c]Not available